

Testing of the RIKEN-ATOMKI CsI(Tl) array in the study of $^{22,23}\text{O}$ nuclear structure

Z. Elekes^{1,2,a}, Zs. Dombrádi¹, S. Bishop², Zs. Fülöp¹, J. Gibelin³, T. Gomi², Y. Hashimoto⁴, N. Imai², N. Iwasa⁵, H. Iwasaki⁶, G. Kalinka¹, Y. Kondo⁴, A.A. Korshennikov^{2,7}, K. Kurita⁸, M. Kurokawa², N. Matsui⁴, T. Motobayashi², T. Nakamura⁴, T. Nakao⁶, E.Yu. Nikolskii^{2,7}, T.K. Ohnishi², T. Okumura⁴, S. Ota⁹, A. Perera², A. Saito⁶, H. Sakurai⁶, Y. Satou⁴, D. Sohler¹, T. Sumikama², D. Suzuki⁸, M. Suzuki⁸, H. Takeda⁶, S. Takeuchi², Y. Togano⁸, and Y. Yanagisawa²

¹ Institute of Nuclear Research of the Hungarian Academy of Sciences, P.O. Box 51, Debrecen, H-4001, Hungary

² The Institute of Physical and Chemical Research, 2-1 Hirosawa, Wako, Saitama 351-0198, Japan

³ Institut de Physique Nucléaire, 15 rue Georges Clemenceau, 91406 Orsay, France

⁴ Tokyo Institute of Technology, 2-12-1 Ookayama, Meguro-ku, Tokyo 152-8550, Japan

⁵ Tohoku University, Sendai, Miyagi 980-8578, Japan

⁶ University of Tokyo, Tokyo 113-0033, Japan

⁷ Kurchatov Institute, Kurchatov sq. 1, 123182, Moscow, Russia

⁸ Rikkyo University, 3-34-1 Nishi-Ikebukuro, Toshima, Tokyo 171-8501, Japan

⁹ Kyoto University, Kyoto 606-8501, Japan

Received: 27 July 2005 /

Published online: 15 March 2006 – © Società Italiana di Fisica / Springer-Verlag 2006

Abstract. The paper reports on the test of the newly developed RIKEN-ATOMKI CsI(Tl) array. It is demonstrated that high-quality detectors with excellent light collection efficiency and narrow resolution distribution could be produced. The setup has been commissioned in the study of the reaction of $^{22}\text{O} + \text{CD}_2$. In the present paper, we summarize the results mainly on the (d, d') channel. From the cross section for the transition between the ground state and the first 2^+ state, we could deduce the “matter” deformation parameter to be $\beta_M = 0.23 \pm 0.02$ by distorted wave analysis. Comparing this data with previous measurements it can be concluded that ^{22}O isotope has moderate and similar neutron and proton deformations.

PACS. 25.70.Hi Transfer reactions – 27.30.+t $20 \leq A \leq 38$ – 29.30.Kv X- and gamma-ray spectroscopy – 29.30.Ep Charged-particle spectroscopy

1 Introduction

The existing and forthcoming radioactive beam facilities open a wide range of possibilities to study exotic nuclei and nuclear processes which play a crucial role in nucleosynthesis. To study direct nuclear reactions of astrophysical and nuclear structure interest in inverse kinematics a light ion spectrometer has been constructed in RIKEN to be applied at the RIBF accelerator facility that is under construction [1].

2 Characterization of the CsI(Tl) detectors

For charged particle detection, CsI(Tl) is an excellent material of choice: it has high light yield; the wavelength of the emitted light (~ 550 nm) matches the sensitivity of silicon photodiodes well; the decay time of the light emission

is a function of the particle type, enabling thereby particle identification. Since CsI(Tl) is only lightly hygroscopic, light reflector wrapping need not to be humidity tight. The only serious drawback of CsI(Tl) is the existence of a long ($\sim 8 \mu\text{s}$) time constant light component. Despite the good light yield, highly efficient and uniform collection of scintillation light from all over the detector volume is mandatory from the point of view of good energy resolution and particle identification alike [2]. This is especially important for low energies where the signal/noise ratio is limited by the inherent leakage current noise of the photodiode. While the necessary thickness of the scintillator is determined by the highest energy of the particles to be stopped in it, the lateral dimensions are dependent on factors like the degree of granularity needed, the size of the photodiode, etc. In our case the detectors are 55 mm thick, making them able to stop charged particles up to 120 MeV/amu, and their cross section is $16 \times 16 \text{ mm}^2$ except for the last 5 mm, where they are tapered to match the $10 \times 10 \text{ mm}^2$

^a e-mail: elekes@atomki.hu

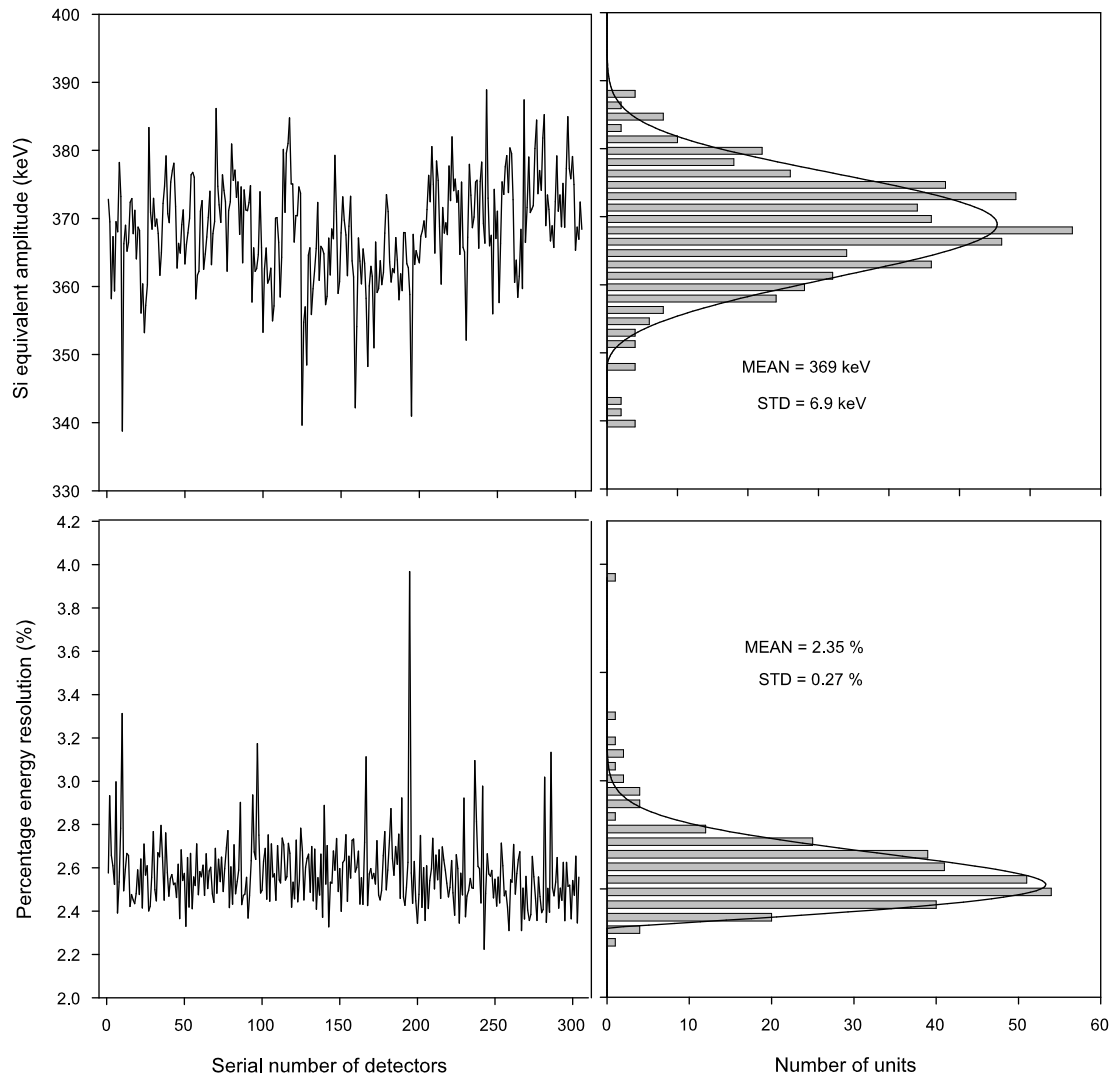


Fig. 1. Distribution of the light collection efficiency and resolution of the detectors.

cross section photodiodes. The light collection efficiency and its uniformity has been optimized through measurements using numerous combinations of different surface conditions and of various wrapping materials for the sides and front face, and also by modeling with Monte Carlo calculations [3]. The best solution for our purpose [4] is front face polished, side surfaces specially depolished and covered with two layers of $60\ \mu\text{m}$ thick VM2000 mirror film [5]. For the front face, this mirror film or thin aluminized Mylar foil can be used, depending on the type and energy of the particles to be detected. Similar solutions in the third generation of DIAMANT detector system [6] in conjunction with Euroball, or in the GLAST space detector system [7], also justifies the choice of this mirror foil as a promising new alternative in scintillation detection to the presently overwhelmingly applied diffuse reflectors.

The quality of the applied technology can be assessed from fig. 1, which summarizes the performance test results obtained with 5.5 MeV alpha particles for all the 312 detector units completed, in the form of amplitude and resolution distribution graphs. The light collection

is so well reproducible that the amplitude distribution is only slightly wider ($\text{FWHM} = 3.2\%$), than the width of an individual spectral peak (2.55%). This means, that practically no gain matching in the array is necessary. During this test all detectors were covered with a thin Aluminized Mylar front reflector. By replacing it with a VM2000 film, which poses no problem in the detection of high-energy light particles, the amplitudes can be increased by $\approx 20\%$, significantly improving thereby the energy resolution. The average value of the low-energy background continuum for 5.5 MeV alphas, not shown in the figure, is less than 3%. It is worth mentioning that despite of the much larger scintillator crystals ($16 \times 16 \times 55\ \text{mm}^3$ vs. $14.5 \times 14.5 \times 3\ \text{mm}^3$) of this system the energy resolution values are only slightly lower (2.5% vs. 2.1%) than that of the DIAMANT system [6]. Please note, that besides charged particles, CsI(Tl) is a sensitive and high-performance gamma ray detector. For gammas, the light yield is ≈ 30 photon/keV with $< 0.3\%$ nonuniformity along the crystal length, whereas the energy resolution for 511 keV is $< 10\%$.

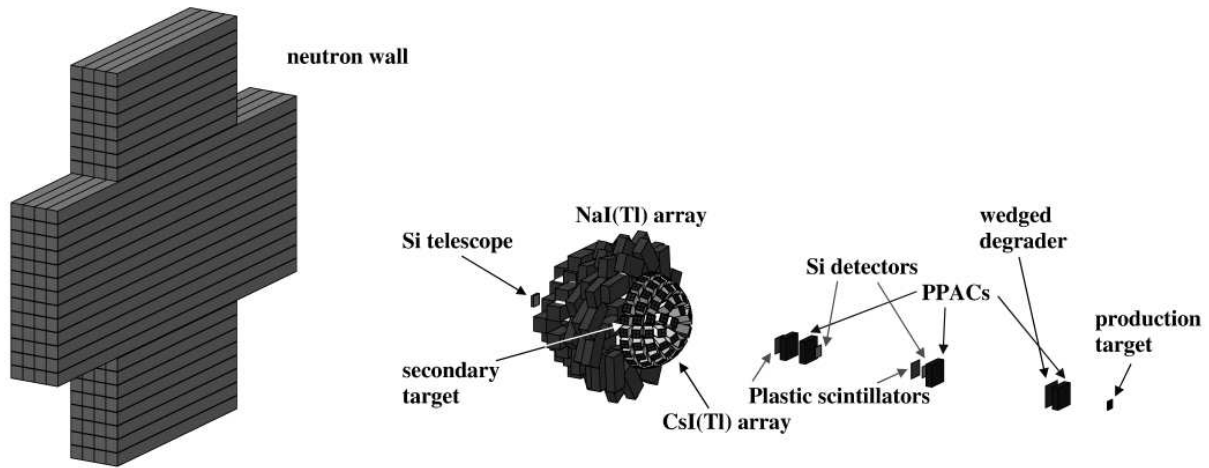


Fig. 2. Schematic view of the experimental setup.

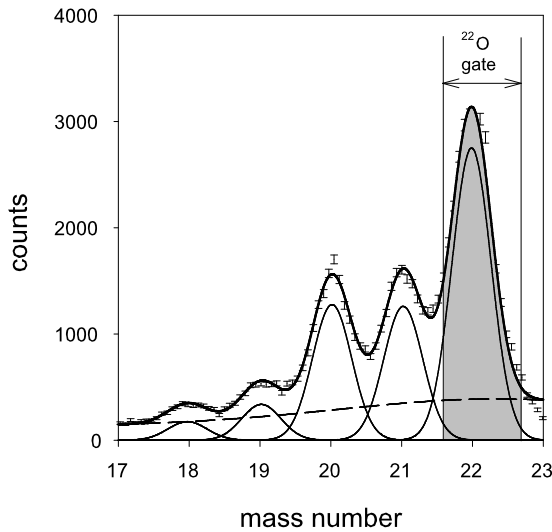


Fig. 3. Separation of oxygen isotopes using ΔE - E information in the silicon telescope. The bold solid line is a sum of 5 Gaussian functions and a polynomial background. The individual Gaussians and the background function are also plotted with thin solid lines.

3 The commissioning experiment

In the commissioning experiment, a 94 A-MeV energy primary beam of ^{40}Ar with 60 pnA intensity hit a ^9Be production target of 0.3 cm thickness. The schematic view of the experimental setup is shown in fig. 2. The reaction products were momentum- and mass-analyzed by the RIPS fragment separator [8]. The secondary beam mainly included neutron-rich ^{25}Ne and ^{22}O nuclei. The RIPS was operated at 6% momentum acceptance. The total intensity was approximately 1500 cps having an average ^{22}O intensity of 600 cps. The identification of incident beam species was performed by energy loss and time of flight. The separation of ^{22}O particles was complete. Two plastic scintillators of 1 mm thickness were placed at the first and

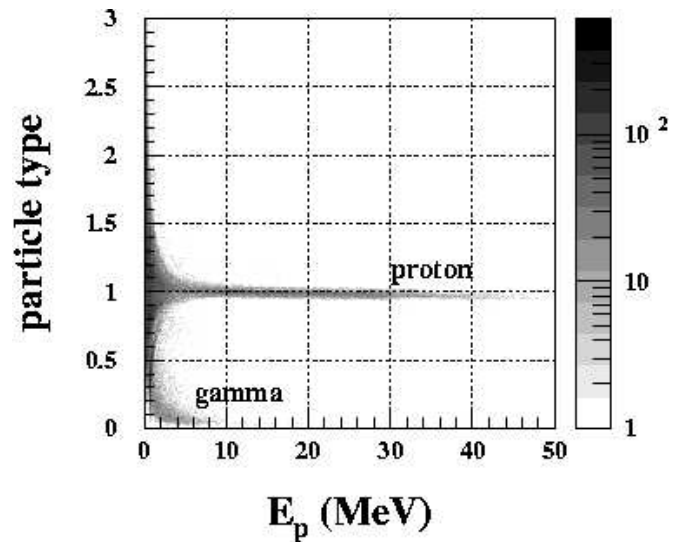


Fig. 4. Particle identification performed by the CsI(Tl) array in coincidence with the incident ^{22}O beam.

second focal planes (F2 and F3) to measure the TOF. Silicon detectors with thickness of 0.5 mm were inserted at F2 and F3 for energy loss determination. The secondary beam was transmitted to a secondary CD_2 target of 30 mg/cm^2 at the final focus of RIPS. The reaction occurred at an energy of 34 A-MeV. The position of the incident particles was determined by two PPACs placed at F3 upstream of the target. The scattered particles were detected and identified by a 2×2 matrix silicon telescope placed 96 cm downstream of the target. The telescope consisted of four layers with thicknesses of 0.5, 0.5, 2 and 2 mm. The first two layers were made of stripped detectors measuring the x and y positions of the fragments. On the basis of ΔE - E information, separation was carried out among the different oxygen isotopes which is demonstrated in fig. 3 where the linearized mass spectrum of oxygen nuclei is shown for one segment of the telescope. The protons emitted backward in the reaction were detected by 156 CsI(Tl)

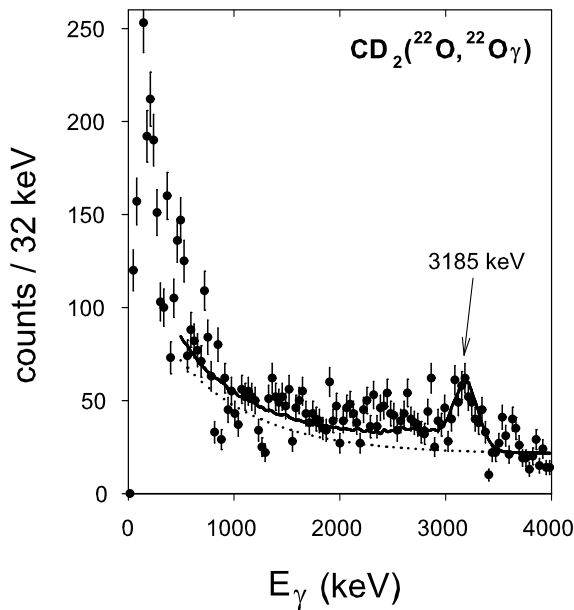


Fig. 5. Doppler-corrected spectra of γ -rays emerging from $^{22}\text{O} + \text{CD}_2$ reaction. The solid line is the final fit including the spectrum curve from GEANT4 simulation and an additional smooth polynomial background plotted as a separate dotted line.

scintillator crystals read out by photodiodes. The particle identification quality is presented in fig. 4 where the gamma rays and protons are well separated from each other down to 1–2 MeV energy of protons. 80 NaI(Tl) scintillator detectors also surrounded the target to detect de-exciting γ -rays emitted by the inelastically scattered nuclei. The intrinsic energy resolution of the array was 10% (FWHM) for a 662 keV γ -ray energy. The neutrons coming from the produced excited ^{23}O nuclei were detected by a neutron wall consisting of four layers of plastic scintillators placed at 2.5 m downstream of the target.

4 Results and discussion

In fig. 5 the Doppler-corrected γ -ray spectra for ^{22}O nucleus is presented, which is produced by putting an additional gate on the time spectra of the NaI(Tl) detectors selecting the prompt events and subtracting the random coincidences. By fitting the spectrum with a Gaussian function and smooth exponential background, first, the position of the single peak was determined at 3185(15) keV. The quoted uncertainty of the peak position is the square root of the sum of the squared uncertainties including two main errors namely the statistical one and the one due to Doppler correction. The above energy for ^{22}O is in a good agreement with the value 3199(8) keV determined earlier [9]. After the peak position has been

determined it was fed into the detector simulation software GEANT4 [10] and the resultant response curve plus a smooth polynomial background was used to analyze the experimental spectrum and determine the cross section for $^{22}\text{O} + ^2\text{H}$ reaction to be $\sigma(0_1^+ \rightarrow 2_1^+) = 19 \pm 3$ mb. From a distorted-wave analysis, we derived the “matter” deformation length (δ_M). In the calculation, the standard collective form factors were applied and the parameter set in [11] was employed for the optical potential. The “matter” deformation length deduced in this way is $\delta_M = 0.77 \pm 0.07$ fm which corresponds to a moderate mass deformation of $\beta_M = 0.23 \pm 0.02$. We can compare this result with the data from $^{22}\text{O} + ^{197}\text{Au}$ reaction [12] where the sensitivity of the probe for proton and neutron distributions is different from that of our case. In the cited work, the proton deformation (β_p) was derived to be between 0.2 and 0.24. This means that the neutron deformation of ^{22}O is very close to that of the proton one taking into account the mass deformation determined in the present study. This result is in contrast with the expectations that the increasing neutron number may lead to a stronger neutron decoupling. In reality, the $M_n/M_p \sim \beta_n/\beta_p$ ratios are 2, 3 and 1 for ^{18}O , ^{20}O and ^{22}O , respectively. The increasing trend is stopped by the $N = 14$ subshell closure, which was indicated already by the high energy of the 2_1^+ state as well as by the small value of the $B(E2; 0_1^+ \rightarrow 2_1^+)$. The subshell closure makes both the proton and neutron distributions nearly spherical in ^{22}O .

We would like to thank the RIKEN Ring Cyclotron staff for their assistance during the experiment. One of the authors (Z.E.) is grateful for the JSPS Fellowship Program in RIKEN and thanks the support from OTKA F60348. The European authors thank the kind hospitality and support from RIKEN. The present work was partly supported by the Grant-in-Aid for Scientific Research (No. 1520417) by the Ministry of Education, Culture, Sports, Science and Technology and by OTKA T38404, T42733 and T46901.

References

1. T. Motobayashi *et al.*, Nucl. Instrum. Methods A **204**, 736 (2003).
2. J. Gál *et al.*, Nucl. Instrum. Methods A **366**, 120 (1995).
3. E. Frlez *et al.*, Comp. Phys. Comm. **134**, 110 (2001).
4. Z. Elekes *et al.*, Nucl. Phys. A **719**, 316C (2003).
5. M.F. Weber *et al.*, Science **287**, 2451 (2000).
6. G. Kalinka *et al.*, ATOMKI Annu. Rep. **64** (2001).
7. <http://glast.stanford.edu>.
8. T. Kubo *et al.*, Nucl. Instrum. Methods B **70**, 309 (1992).
9. M. Stanoiu *et al.*, Phys. Rev. C **69**, 034312 (2004).
10. S. Agostinelli *et al.*, Nucl. Instrum. Methods A **506**, 250 (2003).
11. R.D. Cooper *et al.*, Nucl. Phys. A **218**, 249 (1974).
12. P.G. Thirolf *et al.*, Phys. Lett. B **485**, 16 (2000).